Available online at www.sciencedirect.com

ScienceDirect

Procedia Structural Integrity 64 (2024) 368–375

Structural Integrity Procedia

www.elsevier.com/locate/procedia

SMAR 2024 – 7th International Conference on Smart Monitoring, Assessment and Rehabilitation of Civil Structures

Bending behavior of RC beams with Fe-SMA strip reinforcement

Julien Michels[a,*], Fabienne Mamié[b], Christoph Czaderski[c], Bernhard Schranz[d]

[a]*re-fer AG, Riedmattli 9, 6423 Seewen, Switzerland*
[b]*Baukonstrukt AG, Bäckerstrasse 40, 8004 Zurich, Switzerland*
[c]*Empa, Überlanstrasse 129, 8600 Dübendorf, Switzerland*
[d]*Sika AG, Tüffenwies 16, 8048 Zurich, Switzerland*

Abstract

This paper presents an experimental investigation on reinforced concrete beams with different slenderness strengthened with unbonded Fe-SMA strips. The retrofitting system acts as an external prestressed tendon with a mechanical anchorage. In a first step, the strips are positioned against the concrete bottom surface and fixed against the concrete substrate with a direct fastening system. Activation and hence prestressing of the strips is performed with a gas torch and a subsequent temperature control. The concrete elements are afterwards subjected to 4-point bending up to failure. The aim of the investigation is to assess the structural behavior of the retrofitted members as well the additional strain and stress development in the Fe-SMA strips under additional loading after prestressing. Stress increase in the external strip resulting from the flexural loading has a direct influence on the failure mechanism in a sense that the ultimate stress is governed by the anchorage resistance. The experimental investigation for instance shows the effect of the beam slenderness and reinforcement ratio on the failure mode.

Peer-review under responsibility of SMAR 2024 Organizers

Keywords: structural strengthening; iron-based shape memory alloy; prestressing; RC structures; slenderness effect;

1. Introduction

Strengthening of existing constructions has gained extensive focus during the last three decades and will remain a highly important pillar in structural engineering, due to both economic and environmental reasons.

* Corresponding author. Tel.: +41 41 818 66 66;
E-mail address: jmichels@re-fer.eu

2452-3216
Peer-review under responsibility of SMAR 2024 Organizers
10.1016/j.prostr.2024.09.265

As carbon emissions are still often directly related to the used material (production) and corresponding transport volumes, repair solutions should combine both efficient intervention techniques and innovative materials. Iron-based shape memory alloys (Fe-SMA) represent one of the latest developments in this field, see Cladera et al. (2014). They allow, with their mechanical characteristics, to actively prestress the existing construction and hence release stresses in both concrete and steel. This advantage positively influences the lifespan of the structure by avoiding unnecessary reconstruction. The shape memory effect (SME) of the alloy allows for regaining part of the initial shape upon heating after a permanent predeformation, see Shahverdi et al. (2018). By anchoring the Fe-SMA element to the substrate, shape recovery is prevented and transformed into a stress recovery acting as a prestressing on the parent structure.

This paper presents a study on unbonded Fe-SMA strips with a mechanical end anchorage used to prestress and strengthen RC beams with different slenderness. One aim of the investigation is to assess the strain development in the Fe-SMA under static loading and its impact on the failure mode. The presented experimental investigation is based on an earlier study demonstrating the feasibility of the repair method, see Michels et al. (2018).

2. Experimental investigations

2.1. Beam geometry and materials

Three different geometrical configurations were tested with the respective reinforcement ratios ρ (defined as $A_s/(h{\cdot}b)$) as given in Table 1, a bottom view is shown in Fig. 1. Beam width b was in all cases 0.5 m. The slenderness λ is defined by the ratio L/h. Aimed concrete resistance class was C30/37, reinforcing steel was of type B500B.

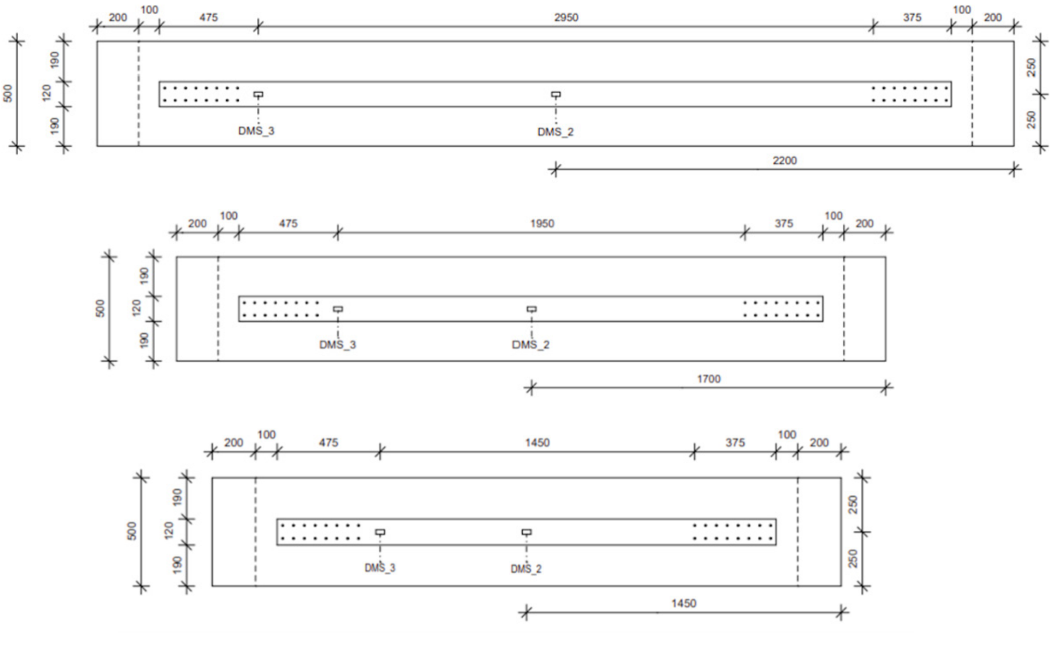

Fig. 1.Geometric configuration (bottom view) for Beams 1, 2, and 3.

Table 1. Beam geometry, reinforcing ratio, and concrete compressive strength on cube on testing day.

Beam	Height h [m]	Span L [m]	Slenderness λ [-]	Reinforc. ratio ρ [%]	Concrete compressive strength cube $f_{c,\text{test}}$ [N/mm^2]
1	0.15	4.0	26.6	0.31	48.5 (±0.8)
2	0.30	3.0	10	0.22	50.5 (±1.2)
3	0.50	2.5	5	0.14	58.5 (±1.5)

2.2. Beam strengthening

Each beam is strengthened with a Fe-SMA strip of type 're-plate' with a width of 120 mm and a thickness of 1.5 mm (see Fig. 1 and 2). Ultimate tensile strength is 750 N/mm^2 at an ultimate strain value of >20%. Maximum loading force and ultimate strain in a structural application is generally governed by the anchorage resistance. The anchorage is composed of at each end 12 direct fasteners of type X-CR 48 P8 S15 (total length 48 mm, penetration depth into concrete ~40 mm) by Hilti. The nails are installed in pairs of 2 along the longitudinal axis at a distance of 30 mm from the lateral strip edge and 50 mm between two subsequent rows. Total anchorage length is hence 250 mm. More information on the anchorage resistance can be found in Empa (2021).

The strengthening of the beam is performed in different steps (see Fig. 2):

- Positioning of the strips in the central axis of the beam.
- Drilling of the concrete through the prepunched ∅4 mm holes in the strip with a ∅3.5 mm drill bit (Fig. 2 left)
- Installing of the X-CR fastener by a powder-actuated setting tool (Fig. 2 middle).
- Activating the Fe-SMA strip in sequential sectors by gas torch with a simultaneous temperature measurement until an activation temperature T_a>300°C is reached, see Fig. 3.

The Fe-SMA strips acts as an external prestressed tendon without bond to the concrete substrate in between the anchorage areas.

Whereas the recovery stress increases with growing maximum activation temperature, 300°C represents a threshold above which no further increase is noticed, Shahverdi et al. (2018). This peak recovery stress is located at 380 N/mm^2, representing an initial total prestress force prior to relaxation of $F_{p,0}$ of 68.4 kN.

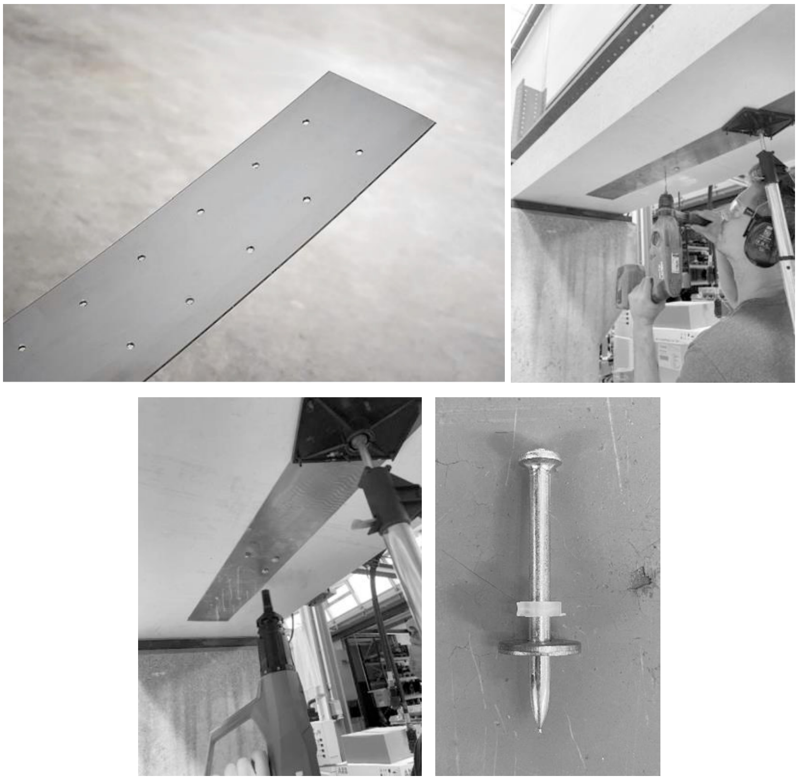

Fig. 2. Fe-SMA strip (upper left), concrete drilling (upper right), X-CR fastener setting (bottom left), X-CR 48 P8 S15 fastener (bottom right).

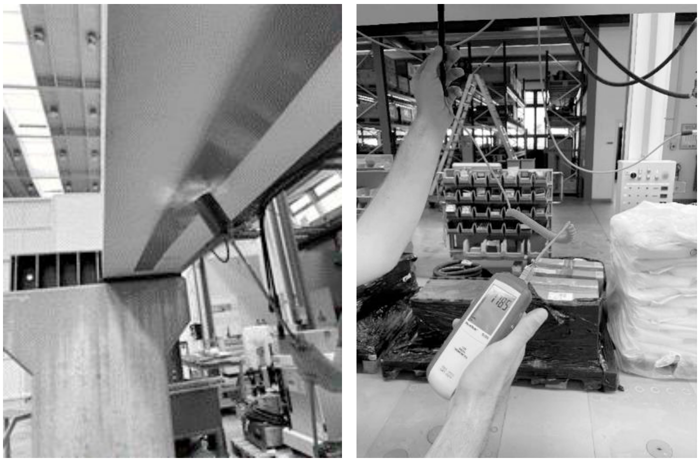

Fig. 3. Strip activation by gas torch (left) and temperature control (right).

2.3. Test setup and loading configuration

The test setup is presented in Fig. 4. The beams are simply supported (one fixed and one rolling end) and loaded in a 4-point bending configuration (indicated loading force *F* corresponds to one loading point). Loading is controlled by vertical displacement (0.03 mm/s in the elastic zone up to cracking and slightly after, 0.3 mm/s up to yielding, and 1 mm/s after yielding up to failure) on one hydraulic jack. Vertical displacement on the beam is measured by two LVDTs placed at midspan. Several loading and unloading stages were included but are not discussed in this paper.

Concrete compressive strain is measured with a strain gauge (DMS1) placed at midspan on the top side, while the Fe-SMA strip is equipped with two strain gauges (DMS2 and DMS3), one at midspan and one at a distance of 475 mm from the strip edge (close to the anchorage).

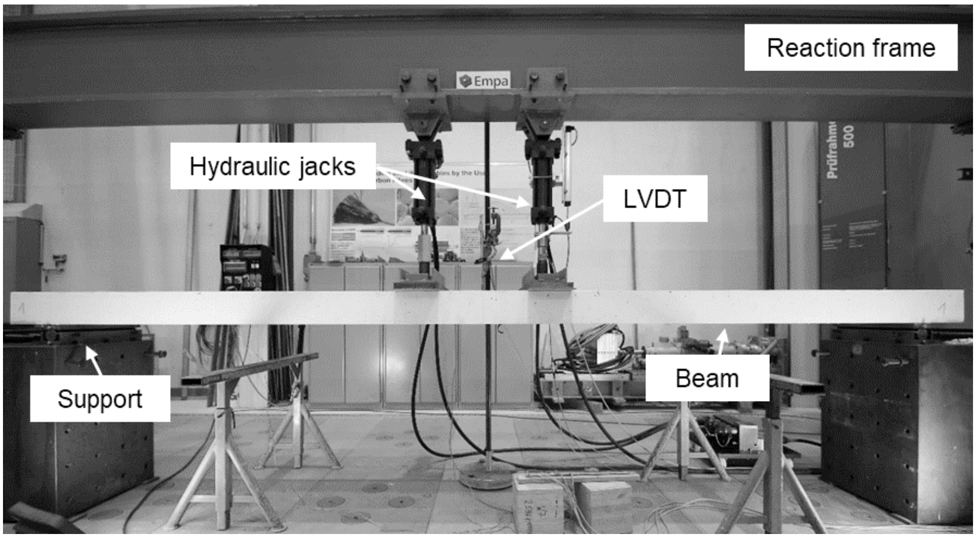

Fig. 4 Test setup for the 4-point bending loading tests.

3. Results and discussion

3.1. Prestressing stage

For Beam 1, the upward deflection u ('-' means the beam moves downwards, '+' means the beam moves upwards) measured with a dial gauge is presented in Fig. 5. The initial negative displacement is due to the thermal expansion of the strip when being heated. After the shape memory effect starts, a tensile force develops in the Fe-SMA strips, prestressing the beam and hence lifting it up.

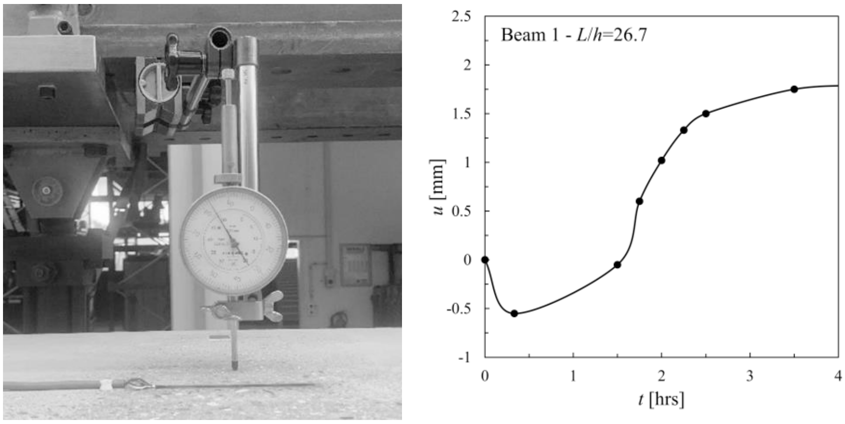

Fig. 5. Uplift u for Beam 1 during activation (heating and cooling).

3.2. Static loading stage

A schematic crack distribution after the test is shown in Fig. 6. Force-deflection and force-strain curves of all performed tests are presented in Fig. 7, experimental results are summarized in Table 1 and 2.. A first observation is the increase of cracking load F_{cr} of the strengthened beam compared to a calculated reference value $F_{cr,0}$ for an unstrengthened beam based on the assumption of a C30/37 tensile strength value of 2.9 N/mm^2, SIA 262 (2013). The maximum bending moment $M_{g,\max}$ at midspan as a result of the dead load g is deducted from the theoretical cracking moment $M_{cr,0}$ (Eq.1). The final reference value $F_{cr,0}$ is obtained by dividing $M_{cr,0}$ by the lever arm L_0 (distance between load introduction point and support), see Eq. 2. Tensile strength of concrete typically exhibits a strong scatter, the calculated reference values are only of indicative nature but can be used for comparison purpose to demonstrate the effect an external prestressing can have.

$$M_{cr,0} = f_{ctm} \cdot W - M_{g,max} \quad (1)$$

$$F_{cr,0} = M_{cr,0}/L_0 \quad (2)$$

Table 1. Summary of experimental results (*at moment of steel bar rupture).

	Beam 1	Beam 2	Beam 3
F_{cr} [kN]	6	30	90
F_y [kN]	13	60	125
F_u [kN]	16.5	70.9	157.8
f_u [mm]	128.1	62.4	26.9
$\varepsilon_{c,u}$ [‰]	-2.25	-3.99	-1.63*
$\varepsilon_{f,u}$ [‰]	6.23 / 5.99	12.74 / 11.13	14.27 / 15.99*
Failure mode	Concrete crushing	Concrete crushing	Steel bar rupture

Table 2. Estimated reference cracking load and experimental observation with Fe-SMA strip prestressing.

	Beam 1	Beam 2	Beam 3
f_{tcm} [N/mm^2]	2.9	2.9	2.9
W [mm^3]	1.88E+06	1.02E+07	2.08E+07
$M_{g,max}$ [kNm]	3.75	4.92	4.88
$M_{cr,0}$ [kNm]	1.69	24.68	55.53
$F_{cr,0}$ [kN] calculated	0.99	20.57	58.46
F_{cr} [kN] experimental	6	30	90

With growing deflection, flexural stiffness of the beams is reduced after reaching the cracking load. Further reduction happens at the yielding point (at F_y) of the inner steel reinforcement. Loading is then continuously increased up to the ultimate failure load.

Failure for Beam 1 and 2 occurred due to concrete crushing at approximately midspan on the upper outside compression fibre. Compressive strain of concrete at failure was -2.25‰ for Beam 1, the crushing location was however outside the measuring range of the strain gauge. For Beam 2, compressive strain was -3.99‰, the strain gauge covering in this case exactly the failure location.

Beam 1 exhibited the highest deflection ductility with f_u =128.1 mm at failure against f_u =62.4 mm for Beam 2. In case of Beam 3, failure occurred due to tensile failure of the inner steel reinforcement, this at a f_u =26.9 mm deflection. As depicted in Fig. 8, significant differences in the Fe-SMA tensile strains at the bottom side could be observed. Whereas at failure load tensile strains $\varepsilon_{f,u}$ for Beam 1 were 6.23‰ and 5.93‰, respectively, Beam 2 strips strains $\varepsilon_{f,u}$ were recorded already at 12.74‰ and 11.13‰, respectively. At failure deflection f_u of 26.9 mm for Beam 3, the corresponding tensile strain in the Fe-SMA is already above 15‰. This is due to the fact, that at equal curvature, an increased section height induces higher strains at the top and bottom fibers. Beam 3 was then further loaded in the post-peak area (loading force approximately 70 kN) up to a load of of 75 kN. After a deflection of bit less than 75 mm, the test was stopped. At that moment, tensile strain $\varepsilon_{f,u}$ in the Fe-SMA strip (strain gauge DM2) was at 26.36 ‰ (strain gauge DMS3 detached at $\varepsilon_{f,u}$ =15.99‰). Also, at these large tensile strains, no anchorage failure occurred.

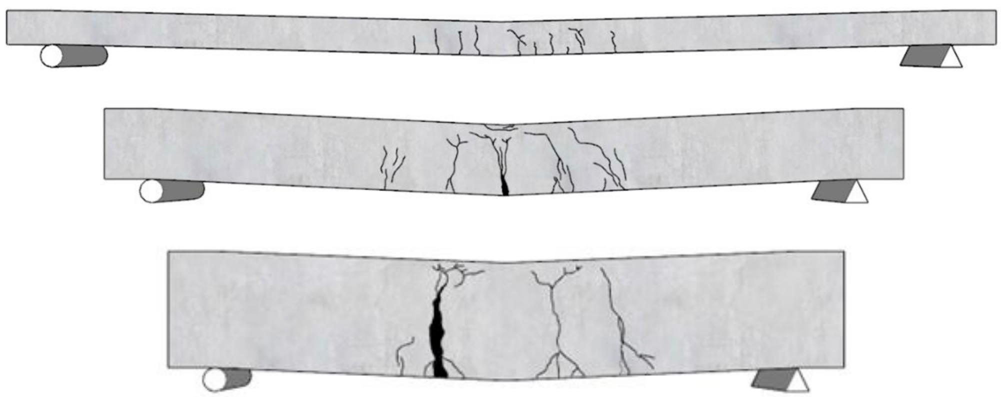

Fig. 6 Crack pattern after test – lateral view.

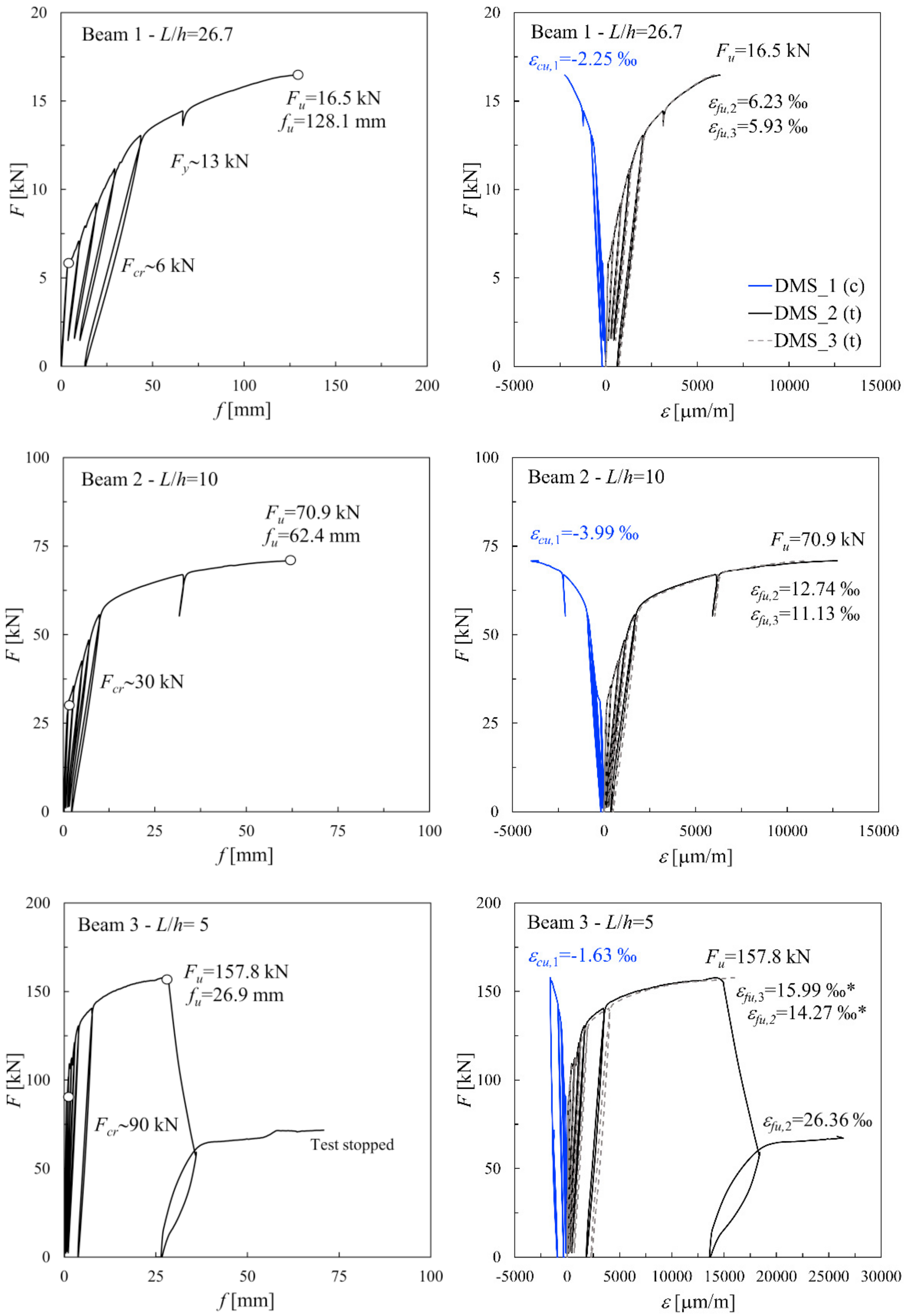

Fig. 7. Force-midspan deflection and force-strain diagrams of Beam 1, 2, and 3 (x- and y-axis not identically scaled, *at moment of steel bar rupture).

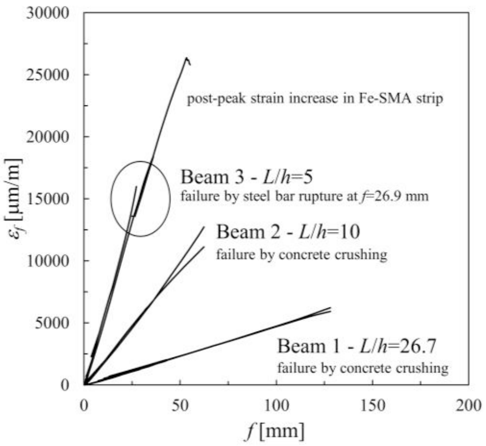

Fig. 8 Strip strain-deflection diagrams of Beam 1, 2, and 3 (for each test, two lines because two strain gauges). .

4. Conclusions and outlook

The following conclusions can be drawn from the presented investigations:

- An iron-based shape memory alloy strip as presented in the current investigation is suitable for structural strengthening both for serviceability and ultimate load purpose.
- The prestressed strip reinforcement increases the cracking and ultimate load compared to a reference structure.
- Beams with high to moderate slenderness and a prestressed strip reinforcement exhibited a very ductile failure, undergoing the classic reinforced concrete stages cracking-yielding-concrete crushing. No anchorage failure occurred.
- The beam with low slenderness exhibited a much faster strain increase in the Fe-SMA strip, but also exhibited an early rupture of the inner steel reinforcement.

Future investigation of both experimental and numerical nature should focus more in detail on the effect of the inner steel reinforcement ratio to deliver further conclusive results for design purpose. Lastly, as the usual analytical methods (e.g. cross-section analysis) cannot be used to calculate externally applied and unbonded strengthening systems the experiments can be used to calibrate calculations tools developed in the past for unbonded steel tendons.

Acknowledgements

Company re-fer AG is acknowledged for providing Fe-SMA memory-steel material as well as assisting during the strengthening of the RC beams. The support of the Empa technical team of the structural testing hall is highly appreciated.

References

Cladera, A., Weber, B., Leinenbach, C., Czaderski, C., Shahverdi, M., Motavalli, M., 2014. Iron-based shape memory alloys for civil engineering structures: An overview, Construction and Building Materials 63, 281-293.

Empa, 2021. Lap-shear tests on X-CR 48 P8 S15 anchorages for re-plate strips. Swiss Federal Laboratories for Materials Science and Technology Test Report No. 52140027302.

Michels, J., Shahverdi, M., Czaderski, C., 2018. Flexural retrofitting of structural concrete with iron-based shape memory strips, Structural Concrete 19, 876-891.

Shahverdi, M., Michels, J., Czaderski, C., Motavalli, M., 2018. Iron-based shape memory alloy strips for strengthening RC members: Material behavior and characterization. Construction and Building Materials 173, 586-599.

SIA 262, 2013. Concrete Structures (design code). Swiss Association of Engineers and Architects.